Supplementary Information

Enhanced green upconversion luminescence in tetrahedral $LiYF_4$:Yb/Er nanoparticles by manganese(II)-doping: The key role of host lattice

Bin Zhou,[a] Bing Xu,[a] Huimei He,[a] Bing Tang,[a] Ying Ma,*[a] Zhanjun Gu,[b] Tianyou Zhai[a]

a. State Key Laboratory of Material Processing and Die & Mould Technology, School of Materials Science and Engineering, Huazhong University of science and Technology, Wuhan 430074, P. R. China.

b. Key Laboratory for Biomedical Effects of Nanomaterials and Nanosafety, Institute of High Energy Physics and National Center for Nanosciences and Technology, Chinese Academy of Sciences, Beijing 100049, P. R. China.

*Corresponding author. E-mail address: yingma@hust.edu.cn

Table S1. Crystallographic parameters of cubic $NaYF_4$ and tetragonal $LiYF_4$ crysals.

Phase	Atom	Site	x/a	y/b	z/c
	Li	4a	0	1/4	1/8
Tetragonal-$LiYF_4$ ($I4_{1/a}$)[1]	Y	4b	1/2	3/4	1/8
	F	16f	0.2815(1)	0.0854(1)	0.0437(1)
	Na	4a	0	0	0
Cubic-$NaYF_4$ (Fm-3m)[2]	Y	4a	0	0	0
	F	8c	1/4	1/4	1/4

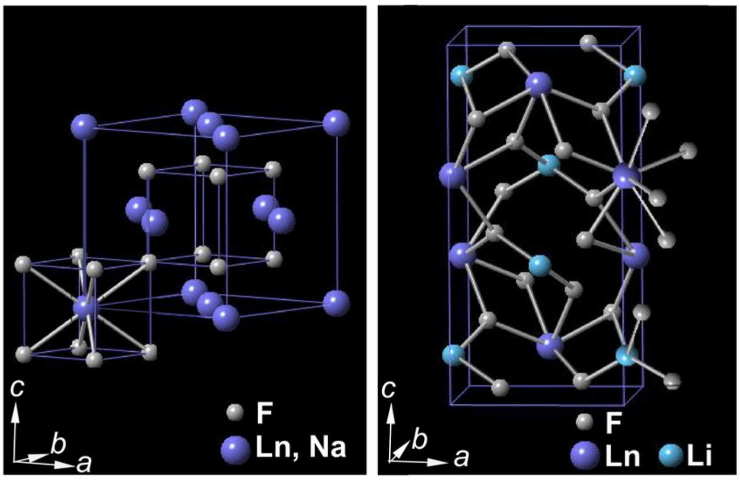

Figure S1. Schematic representation of cubic-phase $NaYF_4$ (left) and tetragonal-phase $LiYF_4$ (right) structure.

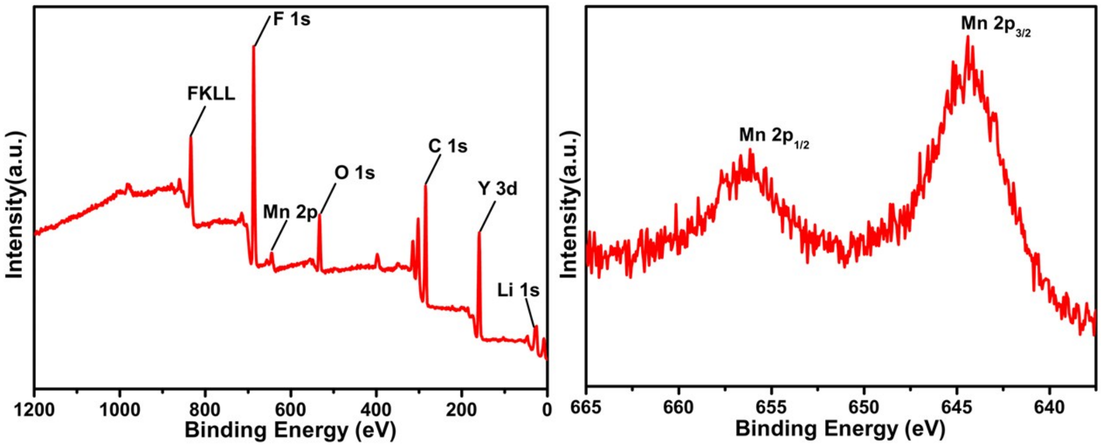

Figure S2 (a) XPS spectrum of Mn^{2+}-doped $LiYF_4$:Yb/Er (20/2 mol%) prepared with 10 mol% feeding concentration; (b) High-resolution XPS spectrum of Mn 2p. The Mn $2p_{1/2}$ and $2p_{3/2}$ signals are located at 654.15 and 642.4 eV, respectively.

Table S2. Elemental analyses of Mn^{2+} in Mn^{2+} doped $LiYF_4$:Yb/Er nanoparticles by ICP-AES measurement.

Nominal concentration (mol%)	**ICP-AES result (mol%)**
5	0.46
8	0.48
10	0.72
12	0.83
14	1.21

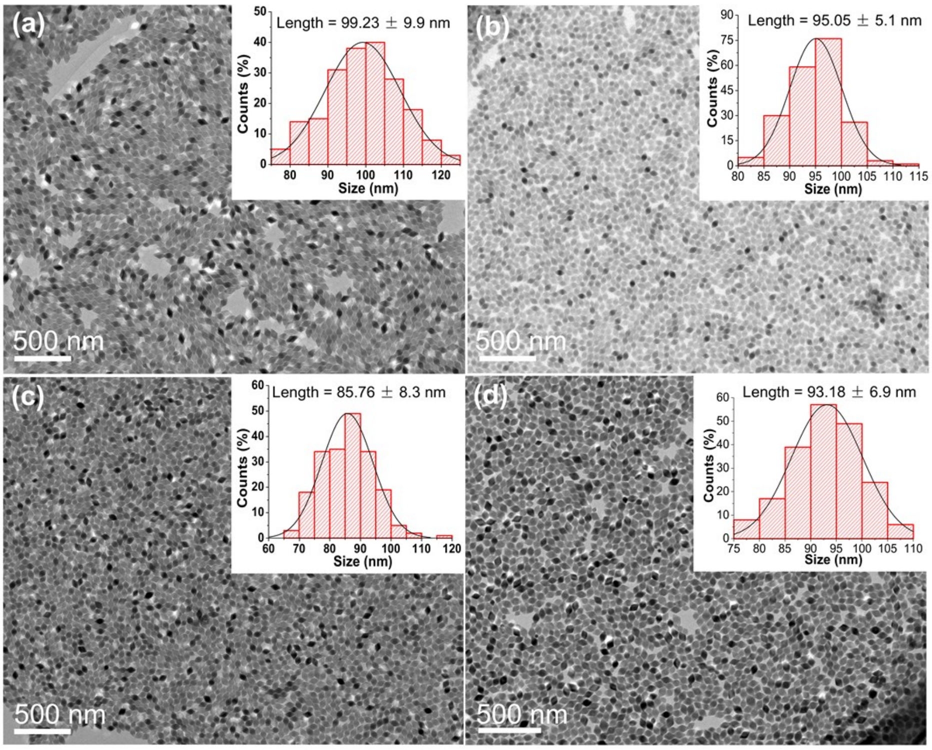

Figure S3. Low-resolution TEM images and the corresponding size distributions of (a) $LiYF_4$:Yb/Er/Mn (20/2/0 mol%), (b) $LiYF_4$:Yb/Er/Mn (20/2/5 mol%), (c) $LiYF_4$:Yb/Er/Mn (20/2/10 mol%) and (d) $LiYF_4$:Yb/Er/Mn (20/2/14 mol%) nanocrystals. The size distributions of the nanocrystals were calculated by counting over 200 particles recorded in the TEM images.

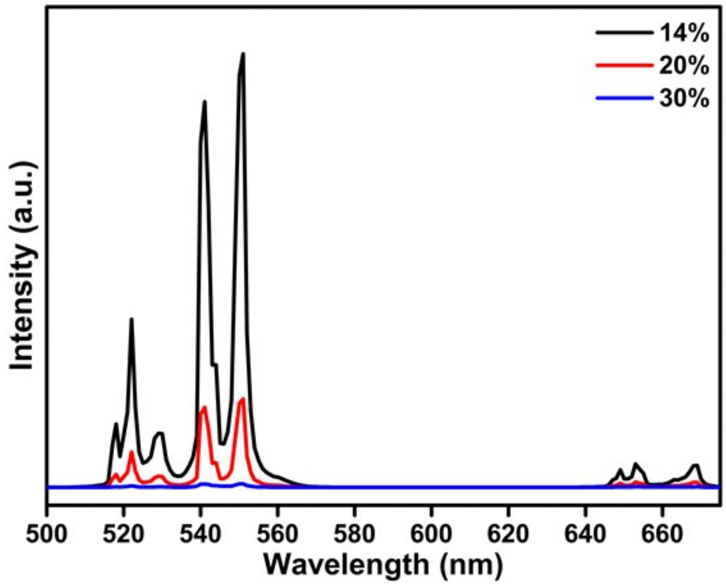

Figure S4. Room-temperature UC emission spectra of cyclohexane solutions containing $LiYF_4$:Yb/Er/Mn (20/2/14-30 mol%) nanoparticles with different Mn^{2+} doping levels, under 980 nm laser excitation (CW, 2 W·cm^{-2}).

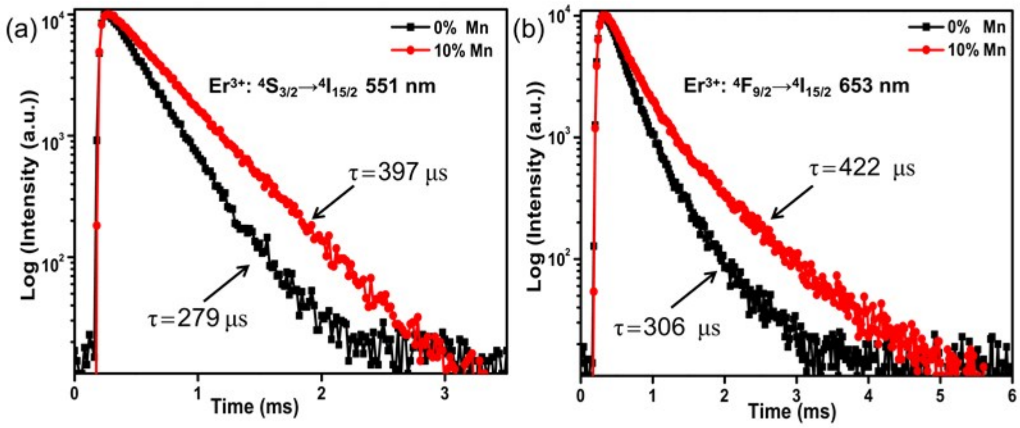

Figure S5. Upconversion luminescence decay curves of Er^{3+} emission at 551 and 653 nm from the $LiYF_4$:Yb/Er nanoparticles with 0 and 10 mol% Mn doping, under pulsed laser excitation at 980 nm.

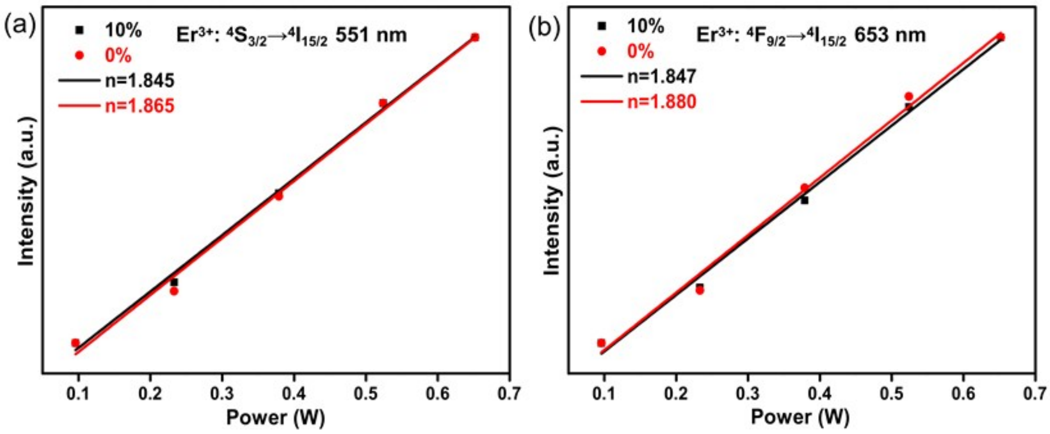

Figure S6. The excitation power dependence of green and red UC emission of $LiYF_4$:Yb/Er (20/2 mol%) NPs with 0 and 10 mol% Mn doping (n represents the numerical value of the slope determined from the linear fitting of the experimental results).

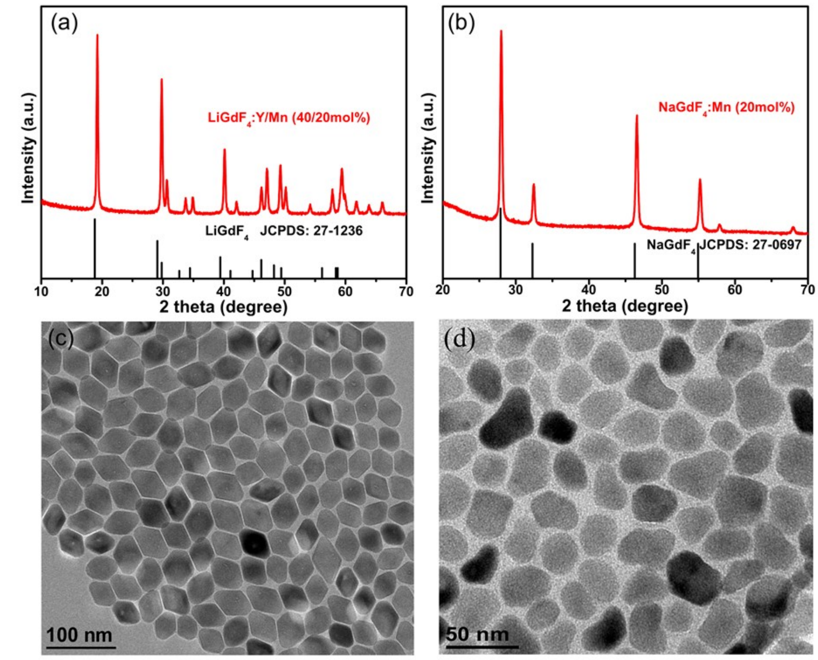

Figure S7. (a-b) XRD patterns and (c-d) TEM images of $LiYF_4$:Gd/Mn (40/20 mol%) and $NaGdF_4$:Mn (20 mol%) nanoparticles.

Table S3. Elemental analyses of Mn^{2+} in $LiYF_4$:Gd/Mn (40/20mol%) and $NaGdF_4$:Mn (10-30 mol%) by ICP-AES measurement.

Sample	**Nominal concentration (mol%)**	**ICP-AES result (mol%)**
$LiYF_4$:Gd/Mn (40/20mol%)	20	1.78
$NaGdF_4$:Mn (30 mol%)	30	2.02
$NaGdF_4$:Mn (20 mol%)	20	1.83
$NaGdF_4$:Mn (10 mol%)	10	0.64

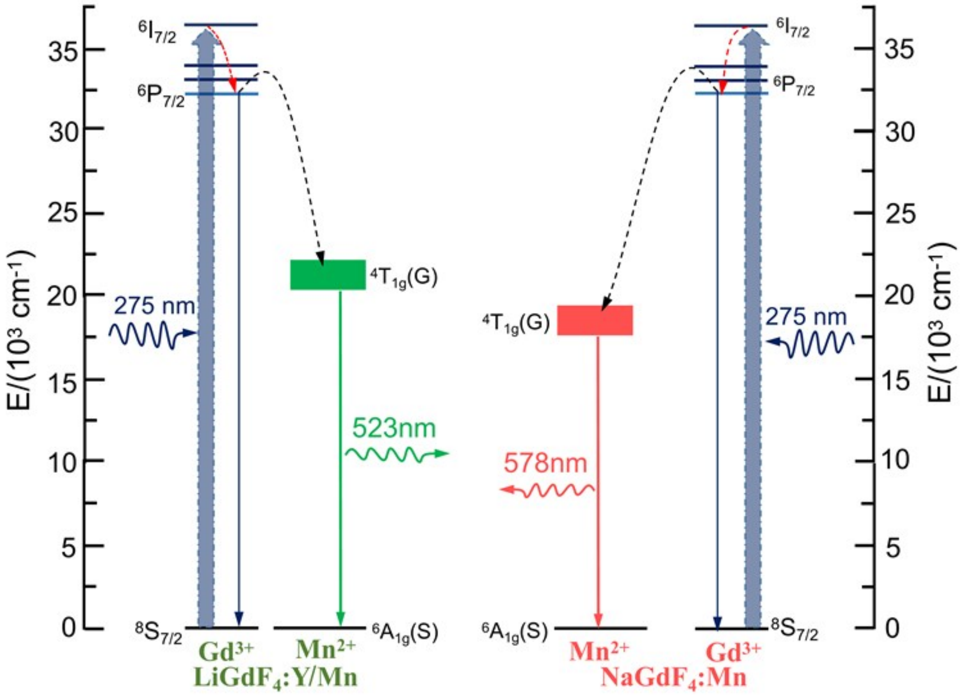

Figure S8. The dominant energy transfer processes in the $LiYF_4$:Gd/Mn (40/20 mol%) (left) and $NaGdF_4$:Mn (20 mol%) (right) nanoparticles.

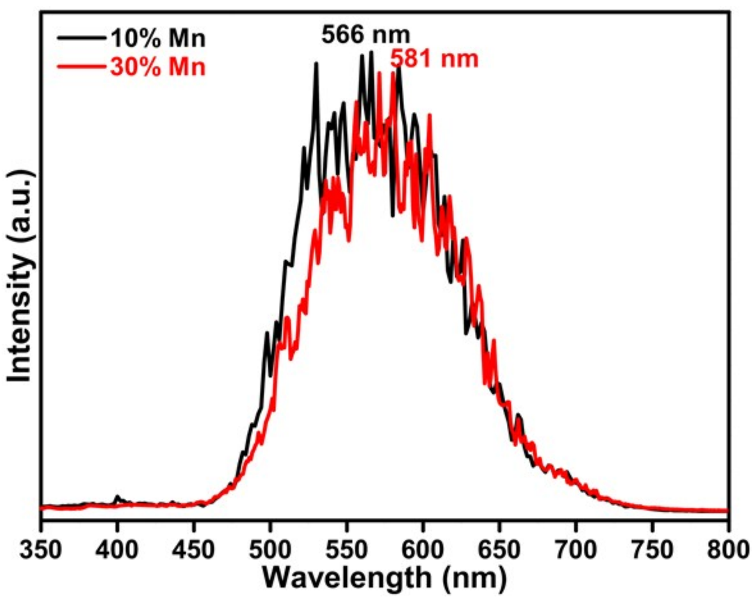

Figure S9. The downconversion emission spectra of the $NaGdF_4$:Mn (10 and 30mol%) colloidal solutions under excitation at 275 nm.

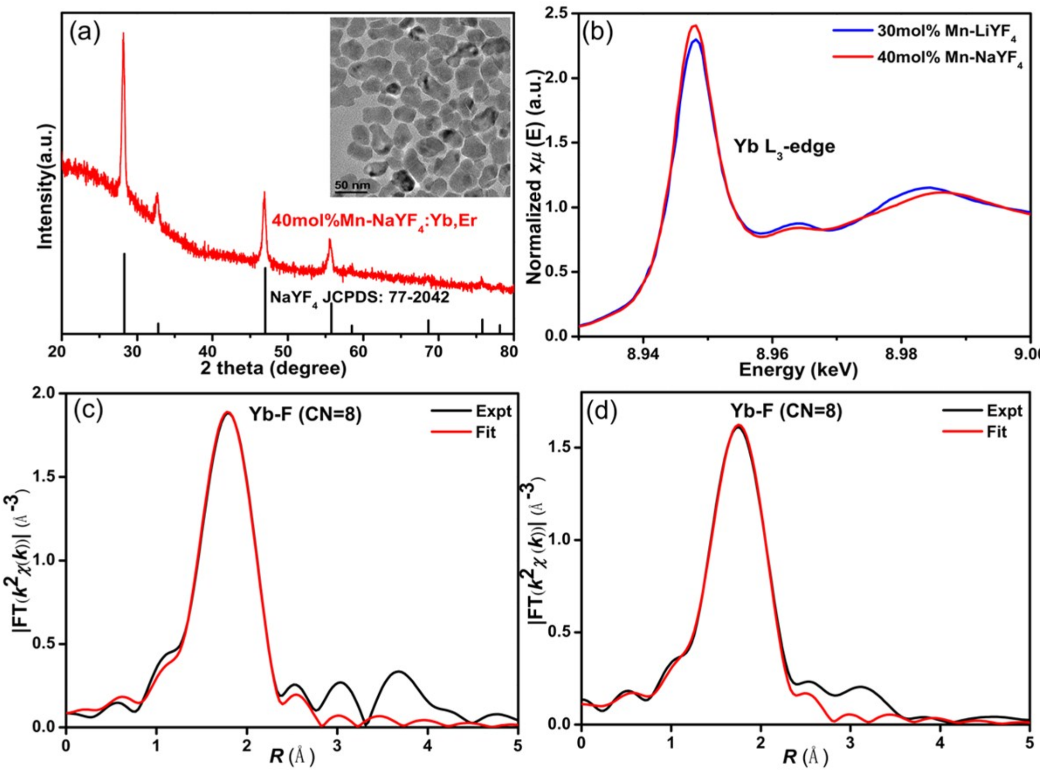

Figure S10. (a) XRD pattern of the as-synthesized $NaYF_4$:Yb/Er nanoparticles doped with 40 mol% Mn^{2+} ions and the standard diffraction pattern of cubic-phase $NaYF_4$ (JCPDS No. 077-2042). Inset shows the TEM image of the corresponding nanoparticles. (b) Yb L_3-edge XANES spectra recorded for 30 mol% Mn-$LiYF_4$:Yb/Er and 40 mol% Mn-$NaYF_4$:Yb/Er nanoparticles. FT k^3-weighted $\chi(k)$-function of EXAFS spectrum for Yb^{3+} in 30 mol% Mn-$LiYF_4$:Yb/Er (c) and 40 mol% Mn-$NaYF_4$:Yb/Er (d) with Yb-F fitting.

Table S4. Yb L_3-edge and Mn K-edge EXAFS curve fitting parameters[a]

sample	chemical bond	CN	R (Å)	σ^2 (Å^2)	ΔE_0 (eV)
30mol%Mn-$LiYF_4$[b]	Yb-F	8.9	2.24	0.007	2.2
	Mn-F	4.1	2.06	0.004	-6.5
40mol%Mn-$NaYF_4$[b]	Yb-F	8.6	2.22	0.010	1.7
	Mn-F	6.1	2.06	0.004	-5.4

[a]CN is the coordination number; R is interatomic distance; σ^2 is Debye-Waller factor (a measure of thermal and static disorder in absorber-scatterer distances); ΔE_0 is the edge-energy shift. Error bounds of the structural parameters were estimated as $N \pm 20\%$; $R \pm 1\%$; $\sigma^2 \pm 20\%$; $\Delta E_0 \pm 20\%$. S_0^2 were fixed to 0.77 for Yb L_3-edge fitting and 0.7 for Mn K-edge fitting. [b]Yb L_3-edge fitting range: $2.0 \leq k$ (/Å) ≤ 8.5 and $1.0 \leq R$ (Å) ≤ 2.4; Mn K-edge fitting range: $2.0 \leq k$ (/Å) ≤ 7.0 and $0.8 \leq R$ (Å) ≤ 2.2.

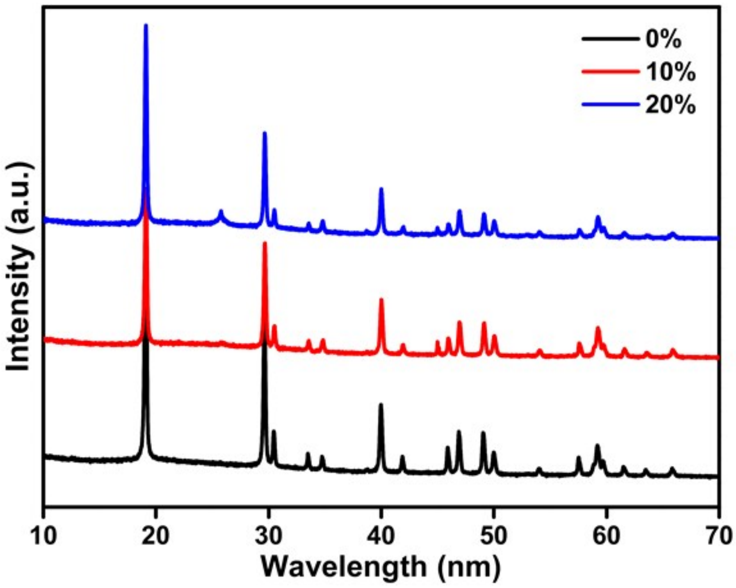

Figure S11. XRD patterns of the as-synthesized $LiYF_4$:Yb/Tm (25/0.5 mol%) nanoparticles obtained in the presence of 0, 10 and 20 mol% Mn^{2+} dopant ions, respectively.

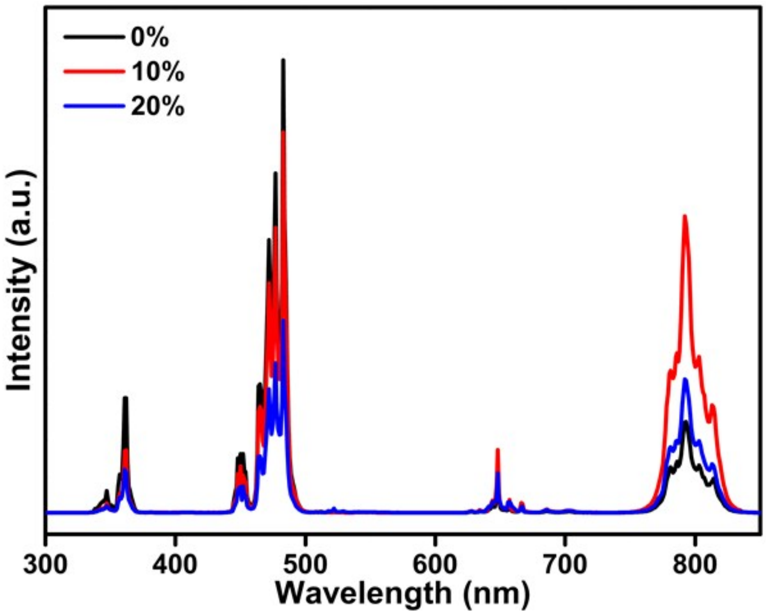

Figure S12. Room-temperature UC emission spectra of cyclohexane solutions containing $LiYF_4$:Yb/Tm/Mn (25/0.5/0-20 mol%) nanoparticles with different Mn^{2+} doping levels, under 980 nm laser excitation (CW, 2 W·cm^{-2}).

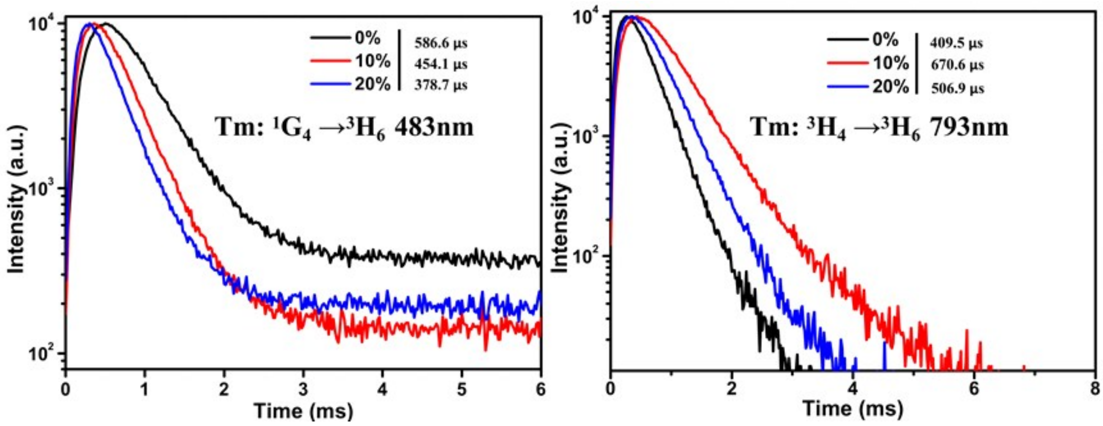

Figure S13. Upconversion luminescence decay curves of Tm^{3+} emission at 483 and 793 nm from the $LiYF_4$:Yb/Tm nanoparticles with 0, 10 and 20 mol% Mn doping, under pulsed laser excitation at 980 nm.

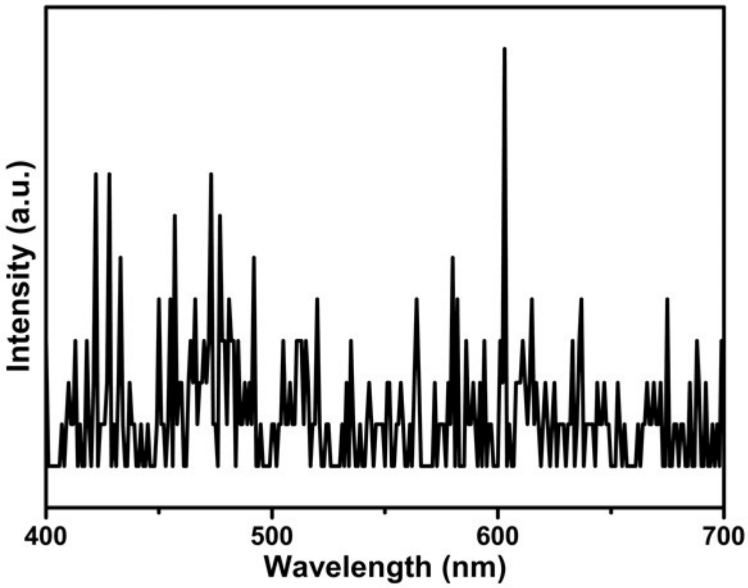

Figure S14. The emission spectra of cyclohexane solutions containing $LiYbF_4$:Mn (10 mol%) nanoparticles at 4K under 980 nm laser excitation.

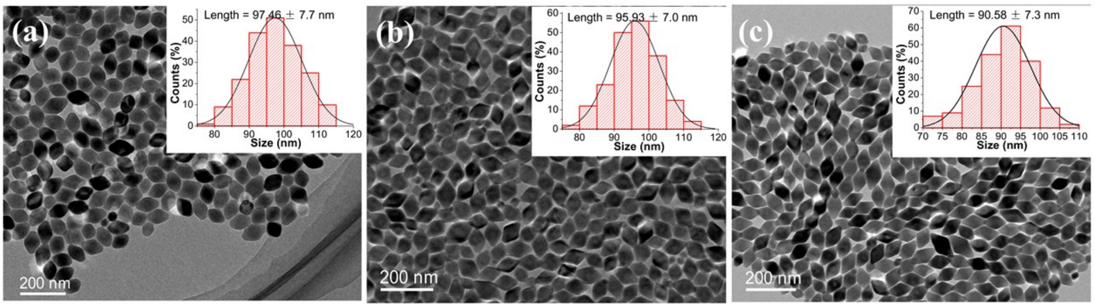

Figure S15. Low-resolution TEM images and size distributions of (a) $LiYF_4$:Er (10mol%), (b) $LiYF_4$:Er/Mn (10/10 mol%) and (c) $LiYF_4$:Er/Mn (10/20 mol%) nanocrystals. The size distributions of the nanocrystals were calculated by counting over 200 particles recorded in the TEM images.

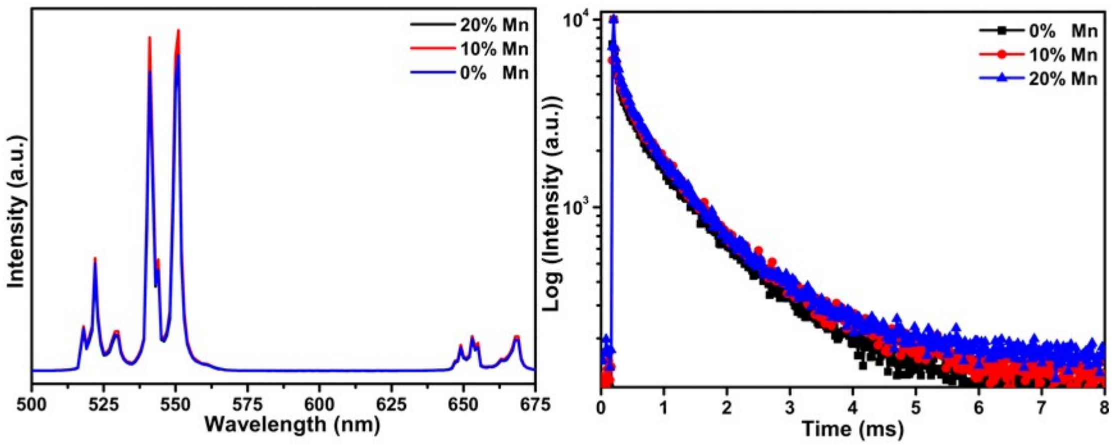

Figure S16. (a) Emission spectra of the $LiYF_4$:Er/Mn (10/0-20 mol%) nanocrystals, under the excitation of 980nm CW laser ($2W\cdot cm^{-2}$). (b) Upconversion luminescence decay curves of Er^{3+} emissions at 551 nm for the $LiYF_4$:Er/Mn (10/x mol%) nanocrystals. Remarkably, the emission intensities and lifetimes of Er^{3+} were found to be independent of Mn^{2+} concentration.

Notes and references

1 D. M. Roy, R. Roy, *J. Electrochem. Soc.*, 1964, **111**, 421-429.

2 A. V. Goryunov, A. I. Popov, N. M. Khajdukov and P.P.Fedorov, *Mater. Res. Bull.*, 1992, **27**, 213-220.